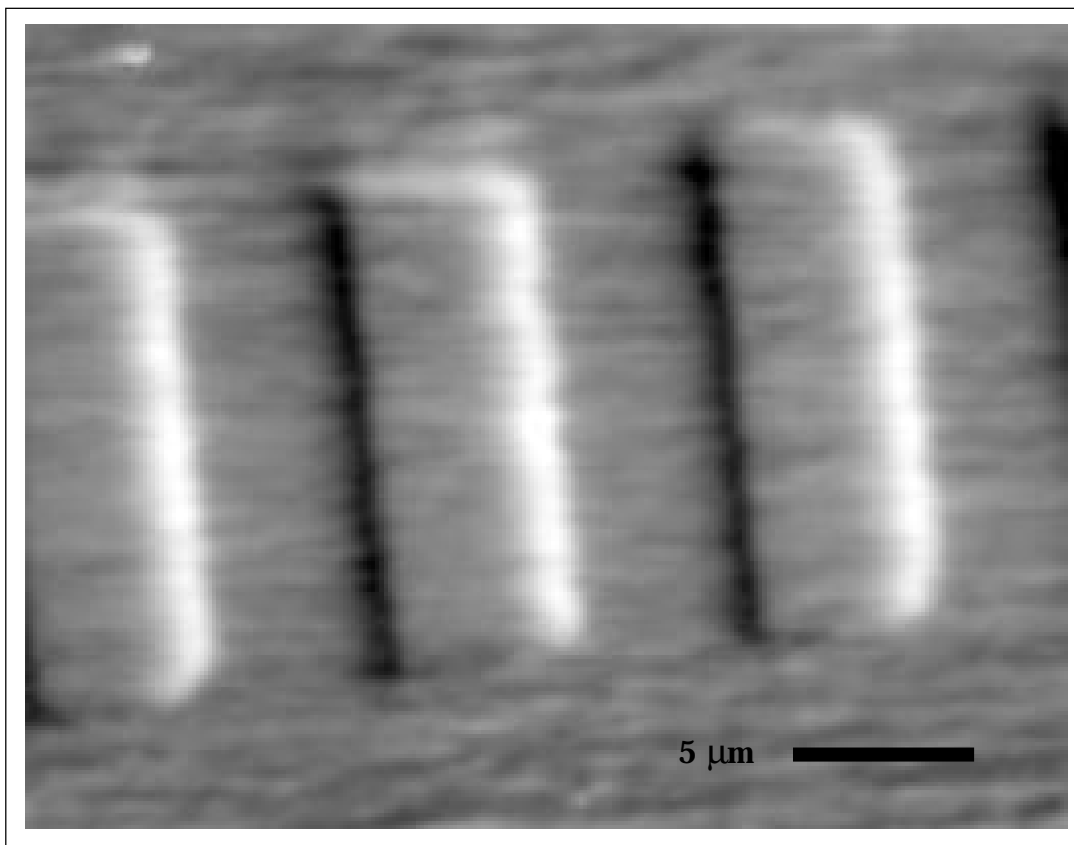


The IRM Quarterly

WINTER 1992-3, VOL. 2, No. 4 INSTITUTE FOR ROCK MAGNETISM

Inside...

Visiting Fellows' Reports	2
Current Abstracts	3
RAC Meeting	7
New Visiting Fellows	8
Best Paper	8



MFM's Miniscule Mechanism Maps Magnetic Moments

Chris Hunt
Roger Proksch
IRM

This article is the fourth and last in our series to explain the use of—and how to use—some of the new pieces of equipment that have added significantly to the capabilities of the IRM during the past year-and-a-half. We hope both to have removed some of the mystique that surrounds these machines, and to have fostered ideas for new experiments afforded by their existence. This time, it's the Magnetic Force Microscope:

1

THE MFM

Our new NanoScope III Atomic/Magnetic Force Microscopy System (AFM/MFM), from Digital Instruments, is the latest in high-tech wizardry. The primary purpose of this versatile surface-analysis tool is to produce images—from atomic-scale maps of the surface topography of a sample, to images of the stray magnetic fields from various types of magnetic materials.

Applications

An AFM/MFM can be used to make direct observations both of the magnetic stray fields from domain walls in magnetic materials, and of the chemical and structural factors involved with domain formation and movement. For example, if a thin section of a rock or a sediment sample is imaged by MFM, it should

be possible, in principle, to observe directly the grains responsible for remanent magnetizations through the stray fields. In fact, *Williams et al. (1992)* have imaged the magnetic stray fields from domain walls in magnetite, and they have attempted to compare the experimental results with micromagnetic calculations [see their abstract, this issue]. While only preliminary, their results suggest that domain walls do not lie parallel to the direction of magnetization in adjacent domains, and that they might even bend near the surface, resulting in magnetic charges appearing on the surfaces of domain walls. Such charges might provide demagnetizing fields strong enough to pin walls at the surface.

Other experimentalists (*Wiesendanger et al., 1992*) have selectively imaged the individual atomic magnetic moments of Fe^{3+} and Fe^{2+} on the A and B sublattice in magnetite [see their abstract, Spring 1992 issue]. This result suggests that it might be possible to detect local ordering in the different magnetic ions, or even to detect exchange-coupling between two different magnetic phases. Detection of the latter is critically important for understanding remagnetization via the chemical remanence (CRM) produced by the magnetite-[or maghemite]-to-hematite transformation. Such work shows the capability of an MFM to help solve fundamental problems in rock magnetism.

Heretofore, the effects of composition, shape, magnetostatic interaction, and stress history on the magnetization of a magnetic phase have been "forward-modeled" and tested by measuring the net magnetization. But now, with a magnetic flux map from an MFM, combined with a chemical-structural map from an AFM, direct tests of the forward models are possible.

continued on page 6...

Visiting Fellows' Reports

We enjoyed working this winter with Visiting Fellow Mr. (soon to be Dr.!) Koji Fukuma from Kyoto University in Japan, who compared pelagic clays from the Pacific with loess and paleosol

Koji Fukuma
Kyoto University

Magnetic properties of Chinese loess and Pacific pelagic clay

My experiments compare the magnetic properties of Chinese loess with those of pelagic clay in the Pacific. Both sediments are believed to be of eolian dust origin blown from central Asia. Previous magnetostratigraphical studies could be well dated nearly up to Matuyama/Gauss boundary for both types of sediment. They share the same magnetic characteristics: alternating field demagnetization is less effective in removing the secondary magnetization compared to thermal demagnetization, and magnetically viscous behavior is high. In addition, since it was recognized that the susceptibility variation of the Chinese loess sequence provides a proxy record of paleoclimatic change, research interest has rapidly increased in recent years. Contrary to the earlier studies, the pedogenic formation of magnetic minerals is now thought to be

David J. Fruit
R. Douglas Elmore
University of Oklahoma

Tectonic components of NRM in folded rocks from northwestern Colorado

In our three-day informal visit to the *IRM* we were able to gather some key elements of data. We are working on the Pennsylvanian Belden Formation on an asymmetric fold in northwestern Colorado. Two magnetic components—an apparently synfolding late Cretaceous component, and a postfolding Ter-

tiary reversed component—are found in most samples. Lithologic factors cause considerable variation in the natural remanent magnetization (NRM) intensity and in the susceptibility from bed to bed.

from China. In addition to the official Fellow, we welcomed a pair of informal visitors, Mr. **David Fruit** and Dr. **Doug Elmore** from the University of Oklahoma, who worked on a Creta-

important to the susceptibility signals. However, compositional and grain-size effects have not been well discriminated in conjunction with pedogenic processes. I have just finished measuring both hysteresis loops on the MicroMag (AGFM), and the temperature dependence of low-temperature remanence using the superconducting susceptometer (MPMS) for some selected samples of Chinese loess. I am thankful for a lot of help from Chris Hunt. Hysteresis measurements are very easy to make, except for being careful of electric sparks between the MicroMag and me. A plastic chair and my sweater are very inductive of electric charges! MPMS can be operated in parallel with MicroMag because this machine is fully automatically controlled and is set in the same room with the MicroMag.

Preliminary results on Chinese loess samples are as follows: (1) Hysteresis properties are quite different between "loess" and paleosol samples. The loess samples have

higher J_r/J_s and H_c , whereas paleosol samples have higher J_s and high-field susceptibilities. (2) Temperature dependence of low-temperature remanence is almost identical in both loess and paleosol; Verwey transitions, indicative of the presence of unoxidized magnetite, are evident for all samples; and no sample shows the Morin transition of hematite.

I have spent just one week of my planned three-week stay at the *IRM*. During my remaining stay, I am going to perform the above type of measurements on pelagic clays from the Pacific, and use the Mössbauer spectrometer to get additional information on magnetic mineralogy. February in Minnesota certainly promises cold and cloudy days, but it is not as miserable as I expected before my visit. No problem arises from the cold weather for measurements in the laboratory at the *IRM*, and I can feel so comfortable except for those electric sparks!

ceous tectonic problem from Colorado. We have prevailed upon our visitors to contribute a summary of work done here at the *IRM*:

I am thankful for a lot of help from Chris Hunt. Hysteresis measurements are very easy to make, except for being careful of electric sparks between the MicroMag and me. A plastic chair and my sweater are very inductive of electric charges! MPMS can be operated in parallel with MicroMag because this machine is fully automatically controlled and is set in the same room with the MicroMag.

Preliminary results on Chinese loess samples are as follows: (1) Hysteresis properties are quite different between "loess" and paleosol samples. The loess samples have

higher J_r/J_s and H_c , whereas paleosol samples have higher J_s and high-field susceptibilities. (2) Temperature dependence of low-temperature remanence is almost identical in both loess and paleosol; Verwey transitions, indicative of the presence of unoxidized magnetite, are evident for all samples; and no sample shows the Morin transition of hematite.

I have spent just one week of my planned three-week stay at the *IRM*. During my remaining stay, I am going to perform the above type of measurements on pelagic clays from the Pacific, and use the Mössbauer spectrometer to get additional information on magnetic mineralogy.

February in Minnesota certainly promises cold and cloudy days, but it is not as miserable as I expected before my visit. No problem arises from the cold weather for measurements in the laboratory at the *IRM*, and I can feel so comfortable except for those electric sparks!



"Lapis polaris magnes"
Engraving by Theodor Galle after Johannes Stradanus;
plate 2 from *Nova reperta*, 17th century

Current Abstracts

A list of current research articles dealing with various topics in the physics and chemistry of magnetism is a regular feature of the IRM Quarterly. Articles published in familiar geology and geophysics journals will be included, but special emphasis is given to current articles from physics, chemistry, and materials science journals. Most abstracts are culled from INSPEC (© Institution of Electrical Engineers), Geophysical Abstracts in Press (© American Geophysical Union), and The Earth and Planetary Express (© Elsevier Science Publishers, B. V.), after which they are edited for the IRM Quarterly. An extensive reference list of articles primarily about rock magnetism, the physics and chemistry of magnetism, and some paleomagnetism is continually updated at the IRM. This list, with nearly 1900 references, is available free of charge. Your contributions both to the list and to the Abstracts section of the IRM Quarterly are always welcome.

Alteration/CRM

Ogishima, T., and H. Kinoshita
Alteration of ferromagnetic components of oceanic basalt under pressurized hydrothermal liquids in laboratory. *J. Geomagn. Geoelectr.*, 44, 309-315, 1992.

Fresh oceanic basalts were altered by heating for several days in a hydrothermal environment (controlled temperature [up to 350°C], pressure [16.5 and 50 MPa], and initial pH). A new magnetic phase formed, as indicated by an irreversible thermomagnetic curve with an apparent Curie point of about 480°C. During further heating in a vacuum, this phase changed into a stable phase with a Curie temperature of about 200°C.

Özdemir, Ö., and D. J. Dunlop
Chemical remanent magnetization during γ -FeOOH phase transformations. *J. Geophys. Res.*, in press, 1993.

Studies were made of chemical remanent magnetization (CRM) accompanying the phase transformations lepidocrocite (γ -FeOOH) \rightarrow maghemite (γ -Fe₂O₃) \rightarrow hematite (α -Fe₂O₃) in a field of 50 μ T at a series of 13 temperatures from 200° to 650°C. Various changes in CRM intensity are explained in terms of phase growth and phase interaction.

Walderhaug, H.
Directional properties of alteration CRM in basic igneous rocks. *Geophys. J. Int.*, 111, 335-347, 1992.

Remagnetization experiments, involving the acquisition of secondary CRM, VRM, and pTRM by reheating in controlled laboratory fields of 0–75 μ T, were carried out on three different basic igneous rocks. Because CRM was acquired when the initially oxidized titanomagnetites were altered under laboratory reheating, identification of primary remanence directions was not possible, despite maximum reheating temperatures well below the original unblocking temperatures.

AMS

Kodama, K. P., and W.-W. Sun
Magnetic anisotropy as a correction for compaction-caused paleomagnetic inclination shallowing. *Geophys. J. Int.*, 111, 465-469, 1992.

Experimental work shows that either randomization or disturbance of sub-vertical magnetite grains causes early inclination-shallowing in sediments. Thereafter, magnetite particles become attached to clay particles, and both magnetic anisotropy and inclination-shallowing increase during compaction. Only the latter part of the compaction process is subject to recognition and correction using an anisotropy of anhysteretic remanence (AAR) technique.

Rochette, P., M. J. Jackson, and C. Aubourg

Rock magnetism and the interpretation of anisotropy of magnetic susceptibility. *Rev. Geophys.*, 30, 209-226, 1992.

When more than one mineral is responsible for magnetic susceptibility, it is impossible to use anisotropy of magnetic susceptibility (AMS) to make quantitative inferences either about preferred orientation of grains or about strain. Therefore, various AMS-specific rock-magnetic techniques must be developed for a better assessment of the geological significance of AMS data. Such techniques will measure susceptibility as a function of both magnetic field and temperature.

Crustal Magnetization

Kikawa, E., and K. Ozawa
Contribution of oceanic gabbros to sea-floor spreading magnetic anomalies. *Science*, 258, 796-799, 1992.

A study of a continuous 500.7-m section of oceanic gabbros (oceanic layer 3) suggests that the magnetic properties of these gabbros, together with the effects of metamorphism and of magmatic evolution, account for a significant part of marine magnetic anomalies.

Toft, P. B., and J. Arkani-Hamed
Induced magnetization of the oceanic lithosphere and ocean-continent magnetization contrast inferred from MAGSAT anomalies. *J. Geophys. Res.*, in press, 1993.

For the oceanic lithosphere in the Iceland plateau, a total induced magnetization of about 2,300 A was determined both from a comparison of calculated anomalies with MAGSAT anomalies, and from rock-magnetic models of the oceanic crust. The total induced magnetization contrast between the nearby Rockall plateau and its surrounding oceanic crust was estimated from MAGSAT anomalies to be about 14,000 A.

Wasilewski, P. J., and M. A. Mayhew

The Moho as a magnetic boundary revisited. *Geophys. Res. Lett.*, 19, 2259-2262, 1992.

A study of globally-distributed xenoliths reinforced the authors' earlier conclusion that, in continental regions, a relatively magnetic crust overlies a relatively non-magnetic mantle. A large upper-mantle xenolith suite of ultramafic composition was characterized by non-magnetic chrome spinels and magnesian ilmenites. In contrast, both prograded crustal rocks, and crustal mafic rocks formed by crystallization at depth, had Curie points of 400°–570°C and were strongly magnetic.

Data Manipulation

Scheepers, P. J. J., and J. D. A. Zijdeveld
Stacking in paleomagnetism: application to marine sediments with weak NRM, *Geophys. Res. Lett.*, 19, 1519-1522, 1992.

A simple stacking routine was used to reduce the scatter in thermal demagnetization results from marine marls and clays; it also made possible the separation of different NRM components in a more consistent and reliable manner. Since the construction of NRM-decay curves was more straightforward, more accurate information about the remanence-carrying minerals could be obtained.

Dating

Özdemir, Ö., and D. York
 $^{40}\text{Ar}/^{39}\text{Ar}$ laser dating of biotite inclusions in a single crystal of magnetite, *Geophys. Res. Lett.*, 19, 1799-1802, 1992.

One half of a 2-mm octahedral crystal of magnetite was subjected to $^{40}\text{Ar}/^{39}\text{Ar}$ laser dating, the other half to scanning electron microscopy (SEM) characterization of crystal inclusions. A 3-D isotope correlation plot reveals a pure radiogenic component corresponding to an age of 323 ± 5 Ma. This is the age of argon closure in minute biotite inclusions, and is thus the minimum age of the magnetite.

Spell, T. L., and I. McDougall
Revisions to the age of the Brunhès-Matuyama boundary and the Pleistocene geomagnetic polarity time-scale, *Geophys. Res. Lett.*, 19, 1181-1184, 1992.

Sanidines, from rhyolites in New Mexico which had been dated by the K-Ar method to establish the age of the Brunhès-Matuyama (B-M) boundary, were re-dated using the $^{40}\text{Ar}/^{39}\text{Ar}$ laser-fusion technique. Results indicate that samples which define the B-M boundary are up to 90 ka older than previously thought, yielding an age for the B-M boundary of 780 ± 10 ka.

Environmental Magnetism

Dekkers, M. J., and H. S. Pietersen
Magnetic properties of low-Ca fly ash: a rapid tool for Fe-assessment and a survey for potentially hazardous elements, *Mater. Res. Soc. Symp. Proc.*, 245, 37-47, 1992.

Rock-magnetic and transmission-electron-microscopy studies show that 20–50% of the total iron in low-Ca fly ashes resides in low-substitution magnetite which occurs as aggregates of closely spaced 10–30-nm spherules. Measurement of magnetic susceptibility might serve as a rapid tool for the evaluation of the speciation of heavy metals in fly ash.

Models

Fukuma, K.
A numerical simulation of magnetostatic coagulation in a fluid, *Geophys. J. Int.*, 111, 357-362, 1992.
The physical and magnetization behaviors of magnetic particles in a fluid were simulated using a Monte Carlo technique which takes into account the effect of magnetostatic interaction between particles. Dilute assemblies show the patterns of magnetization expected from analytical solutions of the non-interacting state. In concentrated assemblies, coagulation occurs, and particle moments in a chain-like cluster are aligned along the chain.

Newell, A. J., D. J. Dunlop, and W. Williams
A two-dimensional micromagnetic model of magnetizations and fields in magnetite, *J. Geophys. Res.*, in press, 1993.

A two-dimensional micromagnetic model was used to obtain magnetic domain structures for cubic magnetite particles having sides of no greater than 1 μm . With increasing particle size, complex submicron structures evolve continuously into recognizable classical domain structures which include both Bloch- and Néel-like walls. There is no critical single-domain size in a conventional sense, but there is a rapid decrease in normalized remanence over the size range 0.06–0.18 μm .

Shcherbakov, V. P., E. McClelland, and V. V. Shcherbakova
A model of multidomain TRM incorporating temperature-variable domain structure, *J. Geophys. Res.*, in press, 1993.

Experimental observations suggested that the dominant controlling factor for TRM acquisition in MD material was the reorganization of domain structure during cooling. A model was developed to satisfactorily explain the experimental observations. The strong effect of thermal pre-history is ascribed to the existence of a spectrum of local energy minima states, and the behavior of an MD grain is likened to that of a spin-glass.

Xu, S., and D. J. Dunlop
Theory of AF demagnetization of multidomain grains and implications for the origin of pseudo-single-domain remanence, *J. Geophys. Res.*, in press, 1993.

Both analytical and numerical models were developed to investigate two factors that affect AF stability in multidomain (MD) grains. It was shown that, because of screening by soft walls, AF stabilities of remanence are usually significantly higher than their micro-coercivities, which are associated with pinned walls.

Paleointensity

Mallioli, J. M., and M. E. Evans
Magnetic intensity variations in red beds of the Lodeve Basin (southern France) and their bearing on the magnetization acquisition process, *Geophys. J. Int.*, 111, 281-290, 1992.
Magnetic intensity in a red-bed sequence from the Permian Lodeve Basin varies by an order of magnitude over stratigraphic distances of only a few centimeters. Intensity peaks are systematically located at bed tops, even though neither the amount nor the properties of the remanence-carrying hematite change. The characteristic intensity patterns can be explained by post-depositional alignment of the grains, with the highest efficiency near the exposed surface.

Meynadier, L., et al.
Relative geomagnetic intensity of the field during the last 140 ka, *Earth Planet. Sci. Lett.*, 114, 39-57, 1992.

Relative geomagnetic paleointensities were obtained from three marine cores from the Somali basin. The remanence intensity was normalized with respect to ARM, with special attention given to changes in grain size, coercivity, and mineralogy. The quasi-cyclic pattern observed during the last 80 ka confirms the results previously obtained from the Mediterranean Sea, and thus establishes the dominantly dipolar character of the field.

Physics

Nikumbh, A. K., A. D. Aware, and P. L. Sayanekar
Electrical and magnetic properties of $\gamma\text{-Fe}_2\text{O}_3$ synthesized from ferrous tartrate one and half hydrate, *J. Magn. Magn. Mater.*, 114, 27-34, 1992.

Maghemite ($\gamma\text{-Fe}_2\text{O}_3$) was analyzed in terms of its DC electrical conductivity, Seebeck coefficient, X-ray diffraction pattern, initial magnetization, magnetic hysteresis, Mössbauer spectrum, and scanning electron microscopy image. Results show that $\gamma\text{-Fe}_2\text{O}_3$ adsorbs oxygen and water from the air, is magnetically single-domain with a six-line Mössbauer spectrum, and is physically acicular.

Polikarpov, M. A., I. V. Trushin, and S. S. Yakimov
Temperature relaxation of a superferromagnetic state in dispersed hematite, *J. Magn. Magn. Mater.*, 116, 372-374, 1992.

Variations in particle packing of dispersed hematite affects its Mössbauer spectrum by causing a reversible transition from a superparamagnetic to a superferromagnetic state as a result of interactions among the magnetization vectors of neighboring particles.

Reversals/VGP paths

Hoffman, K. A.

Dipolar reversal states of the geomagnetic field and core mantle dynamics, *Nature*, 359, 789-794, 1992. The two inclined dipolar field configurations that have dominated the reversal process for the past 10 Ma provided a way to explain the directional rebounds, aborted reversals, and what appear to be preferred VGP reversal paths recorded in sediments. These orientations correlated both with near-radial flux concentrations recognizable when today's field is stripped of its axial dipole, and with lower-mantle seismic anomalies, all of which suggested a tie to deep-Earth dynamics.

Laj, C., *et al.*

Statistical assessment of the preferred longitudinal bands for recent geomagnetic reversal records, *Geophys. Res. Lett.*, 19, 2003-2006, 1992.

Recent polarity reversal records showed a preponderance of transitional VGPs over the Americas and their antipode. Tests using circular statistics showed that this distribution is not consistent with the statistical fluctuations of a random probability distribution; thus, the longitudinal bias requires a physical explanation.

Marzocchi, W., and F. Mulargia

The periodicity of geomagnetic reversals, *Phys. Earth Planet. Inter.*, 73, 222-228, 1992.

Periodogram analysis was used to analyze the periodicities in geomagnetic reversals. The results indicate that reversals since 85 Ma BP occur according to a generalized Poisson process which has an exponentially increasing mean and possibly a superimposed periodic modulation. This is consistent with reversals originated by cyclones in the outer core, a long-term change in the lower mantle temperature distribution, and a pulsating 8-10-km-thick layer at the base of the mantle.

Ohno, M., and Y. Hamano

Geomagnetic poles over the past 10000 years, *Geophys. Res. Lett.*, 19, 1715-1718, 1992.

Locations of the geomagnetic poles over the past 10 ka were calculated by averaging the VGP positions obtained from paleomagnetic data. The distribution of poles was elongated parallel to the longitudinal meridians of 45° and 225°; westward movement of the pole was predominant throughout this period. The results of the last 2 ka are consistent with the geomagnetic poles calculated from archaeomagnetic data.

Weeks, R., *et al.*

Sedimentary records of reversal transitions—magnetization smoothing artefact or geomagnetic field behaviour?, *Geophys. Res. Lett.*, 19, 2007-2010, 1992.

Smoothing over unrealistically long time-scales is required to generate (p)DRM directions which are mixtures of pre- and post-transitional directions. Sedimentary records showing VGP paths in the planes of pre- and post-transitional VGPs can be explained by the non-axisymmetric bias in the non-reversing field, which plays a role in reversals. Thus, proper cleaning to get primary magnetizations will yield true field behavior; otherwise, artifacts can be found.

Rock Magnetism

Halgedahl, S. L.

Experiments to investigate the origin of anomalously elevated unblocking temperatures, *J. Geophys. Res.*, *in press*, 1993.

A study was made of viscous remanent magnetization (VRM) acquired at 225°C by 1-2 μm magnetite particles synthesized by the glass-ceramic method. The results indicate that existing theory cannot satisfactorily account for anomalously high unblocking temperatures. The data do suggest that the thermal response of the domain structure, as determined by thermomagnetic history, plays a critical role in the thermal unblocking process.

Moskowitz, B. M.

High-temperature magnetostriction of magnetite and titanomagnetites, *J. Geophys. Res.*, 98B, 359-371, 1993.

Magnetostriction constants λ_s of synthetic polycrystalline magnetite and titanomagnetite ($\text{Fe}_{3-x}\text{Ti}_x\text{O}_4$, $0 \leq x \leq 0.60$) were measured from 25°C to the Curie temperature T_C . The thermal dependence of the polycrystalline magnetostriction constant $\lambda_s(T)$ varies as $(1-T/T_C)^{1.3}$ for titanomagnetites and as $(1-T/T_C)^{0.9}$ for pure magnetite. It is well approximated by a power-law equation, $\lambda_s(T) \propto M_s^n(T)$, where M_s is the saturation magnetization, and n varies from 2.3 to 3.5 with titanium content.

Özdemir, Ö., and B. M. Moskowitz
Magnetostriction in aluminum-substituted titanomagnetites, *Geophys. Res. Lett.*, 19, 2361-2364, 1992.

Magnetostriction constants λ_s of sintered polycrystalline aluminum-substituted titanomagnetites ($\text{Fe}_{2.4-\delta}\text{Ti}_{0.6}\text{Al}_\delta\text{O}_4$, $0.05 \leq \delta \leq 0.20$) were measured from 25°C to their Curie temperatures T_C . Cell-edge, saturation magnetization M_s , T_C , and λ_s all vary with aluminum concentration. The thermal dependence of the constant $\lambda_s(T)$ is approximated by a power-law equation, $\lambda_s(T) \propto M_s^n(T)$, where n varies from 2.72 to 3.60 with aluminum substitution.

Williams, W., *et al.*

Magnetic force microscopy imaging of domain walls in magnetite, *Geophys. J. Int.*, 111, 417-423, 1992. A magnetic force microscope was used to obtain high-resolution images of the stray magnetic fields on the polished surface of a natural crystal of magnetite. From these images, models were constructed of the magnetic domain boundaries which control the stability of magnetic remanence in multidomain grains. The experimental data favors a Bloch-wall geometry, but it is possible that wall-bending to form a Néel-wall cap can occur within about 20 nm of the grain surface.

Techniques

Devignes, G., V. Barthès, and A. Tabbagh

Direct determination of the natural remanent magnetization effect in a hole drilled in layered ground from magnetic field and susceptibility logs, *Geophys.*, 57, 872-884, 1992.

A new method allows the joint interpretation of both electromagnetic (EM) and magnetic logs in layered ground. Fourier transforms are used to extract from the two signals the magnetic field due to remanence. Theoretical models, supported by results from sedimentary examples, show that remanence can be recovered even if the Koenigsberger ratio is on the order of 0.2, and the thickness of magnetized layer is on the order of 1 m.

Pozzi, J. P., *et al.*

Downhole magnetostratigraphy in sediments: comparison with the paleomagnetism of a core, *J. Geophys. Res.*, *in press*, 1993.

The magnetostratigraphy of weakly magnetized sediments is determined from direct downhole measurements of remanence and susceptibility. Since there is good correlation between the magnetostratigraphy deduced from paleomagnetic measurements performed on 240 standard plugs and that obtained by logging, downhole magnetostratigraphy proves to be a reliable technique; it also has the advantage of yielding continuous data from a large volume of rock scrutinized *in situ*.

Tsokas, G. N., and C. B. Papazachos
Two-dimensional inversion filters in magnetic prospecting: application to the exploration of buried antiquities, *Geophys.*, 57, 1004-1013, 1992.

The majority of exploration target structures at archaeological sites can be represented as assemblages of vertical-sided finite prisms. Using the anomaly of such prisms, the inverse of the shape function is thus computed in the Wenner mode. A filtering scheme results in anomalies which are centered at the epicenter of the disturbing bodies, which delineate their lateral extent fairly well, and which give a measure of their magnetization. ■

... **MFM** continued from page 1

As an initial demonstration of the capabilities of the newest instrument at the **IRM**, a study of many images of CoCr hard-disk material was made. (Though not geologic, such samples were ideal for the initial testing because the domain structure could be easily controlled. In this particular case, the magnetic domains were the "bits"—the 1's and 0's—which form the basis of information in a computer. The bits had been formed with a recording head, the sort one would find in a hard-disk drive.) The results of the study are shown on the cover of this issue: a dramatic image of a single track of written bits.

How?

A little over six years ago, the first Atomic Force Microscope (AFM) was developed by IBM-Zürich's Gerd Binnig, who received the Nobel Prize for his efforts. The device consists of a flexible, sharp, non-conducting tip on the end of a cantilever which scans across a surface [see schematic diagram below]. The vertical motion of the cantilever, as it responds to surface forces, can be measured with such high precision that atomic-scale resolution of a surface can be achieved. There are two basic modes of AFM operation: contact and non-contact. When the AFM is operated in the contact mode, the tip functions as a sensitive profilometer, and the images produced are closely related to surface topography. In the non-contact mode, the tip is scanned some distance above the sample surface, yielding an image of longer-distance forces.

The Magnetic Force Microscope (MFM) is a variation of the non-contact AFM. The main difference between the two is that the tips of the MFM are constructed from, or coated with, a ferromagnetic material that sensitizes them to microscopic magnetic fields. The theoretical lateral resolution in the MFM mode is about 50–100Å, which is well beyond the resolution of most other magnetic imaging techniques. (To date, a resolution of about 500Å has been attained at the **IRM**.)

Principles of Operation

As the cantilever is scanned over the sample surface, its resonant frequency—typically in the range 75–500 kHz—is shifted by the interactions between the sample and the tip of the cantilever. The motion of the tip is measured with light from a laser diode which reflects off of the tip of the cantilever and into an interferometer detector. The system's electronics then use the signal from the detector to determine the shift in the resonant frequency, which in turn is used to form a map of the relative strengths of the tip/surface interactions. This image can then be interpreted in terms of both the topographic and magnetic features of the sample.

There are myriad subtleties which must be taken into account when imaging with the MFM. For instance, when choosing a tip, the interactions between the sample's stray fields and the tip's magnetization, as well as those between the tip's stray fields and the sample's magnetization, must be considered. If the stray fields are too large, either the tip or the sample will be affected

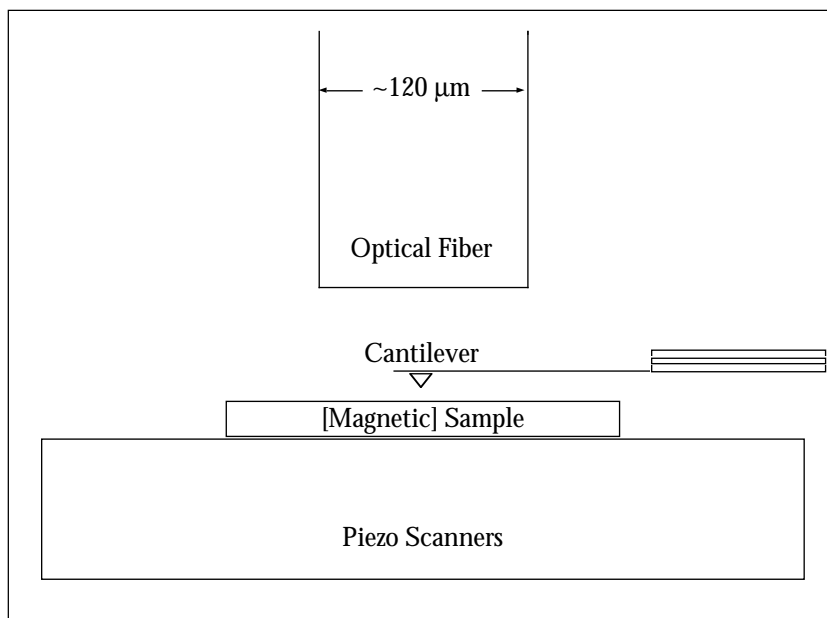
(i.e., remagnetized). To avoid this, the stray fields of the tips must be less than the coercive force of the sample, and the stray fields from the sample must be less than the coercive force of the tip. On the other hand, it is desirable to have as large a magnetic tip moment as possible in order to maximize the signal. For high resolution, it is also important for the tip material to be as localized as possible. A good balance of all these factors has been attained through the use of thin-film tips. Thin films both localize the moment of the tip for higher resolution, and reduce the stray fields of the tip by minimizing the amount of magnetic material there. By a suitable choice both of tip moment and of direction of magnetization (parallel or perpendicular to the sample plane), it is possible to pick out the x-, y-, or z-components of the stray fields of the sample, and map them over the surface.

Another thing to take into account is that competing interactions make image acquisition and interpretation difficult. For example, the presence of electric and van der Waals' forces—topographic forces—affects the MFM during operation. When these forces combine with magnetic forces, the result is a complex convolution of surface topography and magnetic signal in the image produced. However, separate images of the topography and the magnetics can nonetheless be obtained by delicate machine manipulation and image processing. (The cover image is a case in point: although the interactions caused by topographic irregularities and scratches in the surface of the sample can still be faintly discerned, those resulting from the magnetic stray fields of the bits dominate the image.)

Nitty Gritty

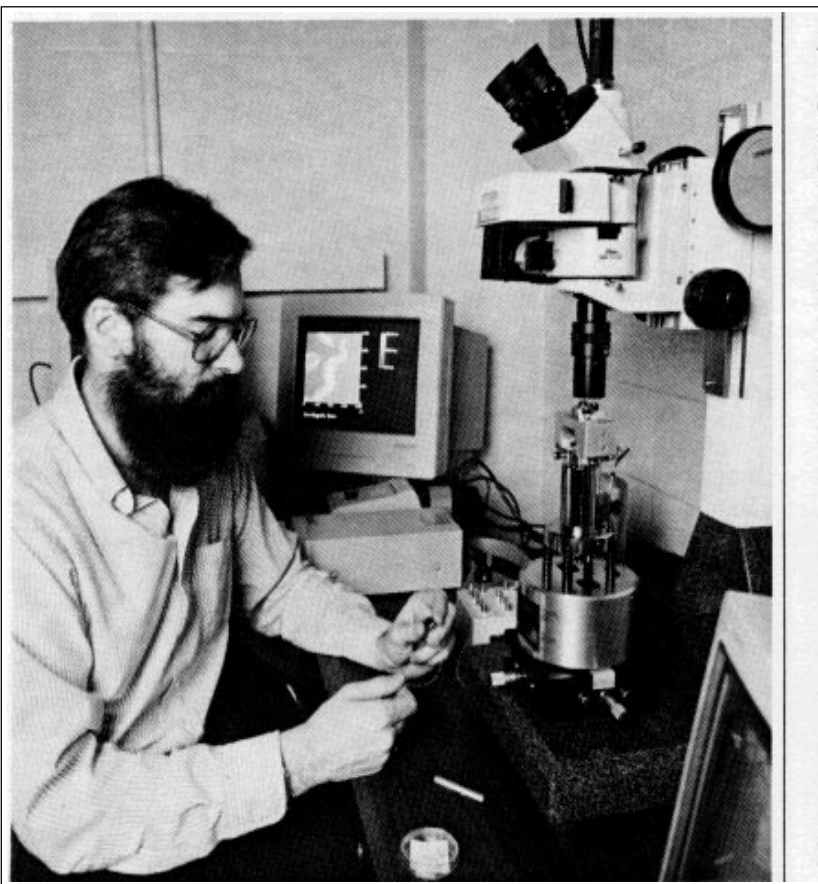
A sample—which consists of a few tens of milligrams of either a magnetic separate, a polished thin section, a piece of magnetic material, or an individual crystal—is placed on the sample holder and the cantilever tip is brought close with the aid of an optical microscope and a video camera. A computer controls the horizontal and vertical positions of the sample, and it processes the signal from the laser diode interferometer as the sample is moved horizontally to produce a gray-scale video image. The actual time required to get a good scan can be

Schematic drawing of an AFM/MFM. The sample is moved back and forth by the piezo scanners. The position of the cantilever, as it interacts with the sample, is monitored via a laser diode interferometer. The signal from the interferometer is converted into a gray-scale image which is a map of the cantilever's topographic, electric, or magnetic interactions with the sample.



Your astute (and hirsute) editor shows that he can pose with a flake of hard-disk material in front of the MFM with an AFM image of a magnetotactic bacterium on the screen behind.

Photo: Chris Faust, Space Science Graphics



anywhere from an hour or so to an entire day, depending upon the perverseness of the sample. The data are also stored as TIFF files, and software permits a dazzling array of data massaging, image manipulation, and plotting options. Then all you need is a printer that you can tie up for half an hour while all the numbers are crunched!

Pluses and Minuses

Because the MFM is quite complicated, with a long and arduous learning curve, it requires an operator with patience and a bent for tinkering. Fortunately, the *IRM* has co-opted a battery of agile graduate students from the Physics Department to do all the work! There is not yet any external field or temperature control, and one must be relatively quiet to keep the machine de-coupled from environmental vibrations.

Yet, the advantages of an MFM over other techniques for magnetic imaging are many: ease of sample preparation, sensitivity to magnetic structures that are below a non-magnetic layer, and operation in almost any medium (vacuum, air, or fluid). In addition, samples do not have to be ultra-clean—a boon with geologic samples. And best of all, it fits on a desk-top.

Addendum

The suspense is over—you can sleep tonight: You were promised an answer to, “Why do all the names for new equipment at the *IRM* begin with the letter ‘M’?” Here goes:

Mercy, don’t imagine for a manic moment merely that machines which make *magnetic measurements* must perforce manifest the letter “M.” My, how moronically mundane and misguided! More mirthfully (and monumentally mendaciously): Manufacturers of magnetic mechanisms methodically muster Madison Avenue Moguls to mastermind their marketing. In the miasmatic maze of mercurial mercantilism, the most meritorious (meretricious?) maneuvers are rewarded by more moolah. The Machiavellian Mavens of Merchandising make much of the mesmerizing effect, the mellifluous appeal of the “M” motif—witness such money-making miracles as Maytag, Marlboro, Mickey Mouse, and (of course!) M&Ms. So, to be competitive, monikers of modern machinery must be magical and mollifying, melodious and marvelous. In other words, it’s all monstrous manipulation! ■

RAC Meets at AGU

The *IRM* Research and Advisory Committee (RAC) held its semi-annual meeting at the AGU conference in San Francisco last December. The agenda included the three-year renewal proposals to our funding agencies (the National Science Foundation and the W. M. Keck Foundation), the timing of advertisements for Visiting Fellowship application deadlines, and the results of the informal survey we did for our progress report.

Among the various parts of the *IRM* renewal proposals discussed were: (1) What types of new equipment should be requested. (Many items were chosen in direct response to the *IRM* survey done last fall [see below].) (2) The efficacy of increasing the Visiting Fellowship travel funds to \$500.

Application deadlines for Visiting Fellowships will now be advertised twice—and with longer lead time—in *Eos*. The possibility of advertising elsewhere (*GSA Today* or *Physics Today*) was also mentioned.

Based on the surveys returned, respondents were very favorable about the *IRM*. Suggestions for improvement included ideas such as putting together an instruction manual or videotape for all *IRM* equipment, and aggressively targeting and recruiting more users.

Two new RAC members—**Chad McCabe** (Louisiana State University) and **Dan Dahlberg** (University of Minnesota)—have replaced outgoing members **Rob Van der Voo** (University of Michigan) and **Mike Sharrock** (3M Corporation) whose two-year terms had run out.

The next RAC meeting will take place in May at the *IRM*. ■

